

See discussions, stats, and author profiles for this publication at: <https://www.researchgate.net/publication/259446066>

# Phase Changes in Mixed Lipid/Polymer Membranes by Multivalent Nanoparticle Recognition

ARTICLE *in* LANGMUIR · DECEMBER 2013

Impact Factor: 4.46 · DOI: 10.1021/la403763v · Source: PubMed

CITATIONS

5

READS

48

5 AUTHORS, INCLUDING:



[Adekunle Olubummo](#)

Martin Luther University Halle-Wittenberg

6 PUBLICATIONS 115 CITATIONS

[SEE PROFILE](#)



[Jörg Kressler](#)

Martin Luther University Halle-Wittenberg

202 PUBLICATIONS 3,352 CITATIONS

[SEE PROFILE](#)



[Wolfgang H. Binder](#)

Martin Luther University Halle-Wittenberg

183 PUBLICATIONS 4,838 CITATIONS

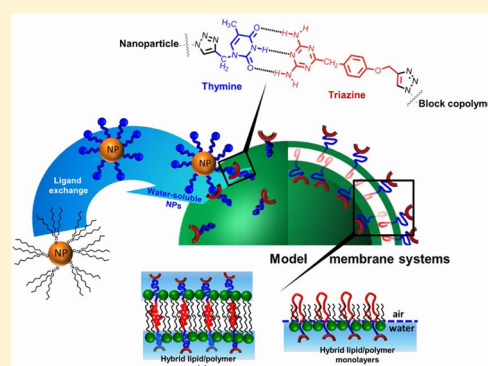
[SEE PROFILE](#)

## Phase Changes in Mixed Lipid/Polymer Membranes by Multivalent Nanoparticle Recognition

Adekunle Olubummo,<sup>†</sup> Matthias Schulz,<sup>†</sup> Regina Schöps,<sup>‡</sup> Jörg Kressler,<sup>‡</sup> and Wolfgang H. Binder<sup>\*,†</sup><sup>†</sup>Chair of Macromolecular Chemistry, Faculty of Natural Sciences II (Chemistry, Physics and Mathematics), Institute of Chemistry, Martin-Luther University Halle-Wittenberg, D-06120 Halle (Saale), Germany<sup>‡</sup>Physical Chemistry, Faculty of Natural Sciences II (Chemistry, Physics and Mathematics), Institute of Chemistry, Martin-Luther University Halle-Wittenberg, D-06120 Halle (Saale), Germany

## S Supporting Information

**ABSTRACT:** Selective addressing of membrane components in complex membrane mixtures is important for many biological processes. The present paper investigates the recognition between multivalent surface functionalized nanoparticles (NPs) and amphiphilic block copolymers (BCPs), which are successfully incorporated into lipid membranes. The concept involves the supramolecular recognition between hybrid membranes (composed of a mixture of a lipid (DPPC or DOPC), an amphiphilic triazine-functionalized block copolymer TRI-PEO<sub>13</sub>-*b*-PIB<sub>83</sub> (BCP 2), and nonfunctionalized BCPs (PEO<sub>17</sub>-*b*-PIB<sub>87</sub> BCP 1)) with multivalent (water-soluble) nanoparticles able to recognize the triazine end group of the BCP 2 at the membrane surface via supramolecular hydrogen bonds. CdSe-NPs bearing long PEO<sub>47</sub>-thymine (THY) polymer chains on their surface specifically interacted with the 2,4-diaminotriazine (TRI) moiety of BCP 2 embedded within hybrid lipid/BCP mono- or bilayers. Experiments with GUVs from a mixture of DPPC/BCP 2 confirm selective supramolecular recognition between the THY-functionalized NPs and the TRI-functionalized polymers, finally resulting in the selective removal of BCP 2 from the hybrid vesicle membrane as proven via facetation of the originally round and smooth vesicles. GUVs (composed of DOPC/BCP 2) show that a selective removal of the polymer component from the fluid hybrid membrane results in destruction of hybrid vesicles via membrane rupture. Adsorption experiments with mixed monolayers from lipids with either BCP 2 or BCP 1 (nonfunctionalized) reveal that the THY-functionalized NPs specifically recognize BCP 2 at the air/water interface by inducing significantly higher changes in the surface pressure when compared to monolayers from nonspecifically interacting lipid/BCP 1 mixtures. Thus, recognition of multivalent NPs with specific membrane components of hybrid lipid/BCP mono- and bilayers proves the selective removal of BCPs from mixed membranes, in turn inducing membrane rupture. Such recognition events display high potential in controlling permeability and fluidity of membranes (e.g., in pharmaceuticals).



## ■ INTRODUCTION

Supramolecular recognition in the form of hydrogen bonds between a guest and a host molecule is one of the most important processes for spontaneous association of molecules under equilibrium conditions into stable structures, well-defined aggregates, and highly organized systems.<sup>1–6</sup> So far, many hydrogen-bonding systems have been studied in organic solvents since hydrogen bonds tend to be weakened considerably in aqueous solution as a result of the competitive binding of water molecules, thus in turn disrupting many hydrogen bonds.<sup>7</sup> However, due to their high specificity, hydrogen bonds exert a significant and still strong binding at interfaces, especially the air/water interface, given that they are affixed to amphiphilic compounds able to guide interfacial assembly. Thus, Langmuir monolayers at the air/water interface have served extensively as a model system for one of the two coupled monolayers in a bilayer membrane to mimic the recognition of hydrogen bonds,<sup>8–10</sup> allowing to specifically

study this molecular recognition between a dissolved guest and a host component.<sup>11,12</sup> A significant number of hydrogen-bonding interactions at the air/water interface have been studied (e.g., those between diaminotriazine (TRI) and thymine (THY) derivatives,<sup>8</sup> amphiphilic orate and adenine,<sup>13</sup> barbituric acid and triaminotriazine,<sup>14</sup> barbituric acid and melamine,<sup>15</sup> adenine and thymine,<sup>16</sup> guanidine/carboxylic acids,<sup>17,18</sup> azobenzene and cyclodextrin,<sup>19</sup> or  $\beta$ -cyclodextrine and cholesterol<sup>20</sup>), revealing the tendency to form relatively complex aggregates with such “simple” molecules. When the interaction between two supramolecular moieties is strong, removal of membrane components takes place showing distinct effects on the membrane organization. Thus, e.g. when  $\beta$ -cyclodextrin ( $\beta$ -CD) interacts with cholesterol in mono-<sup>21–23</sup>

Received: October 5, 2013

Revised: December 9, 2013

Published: December 12, 2013



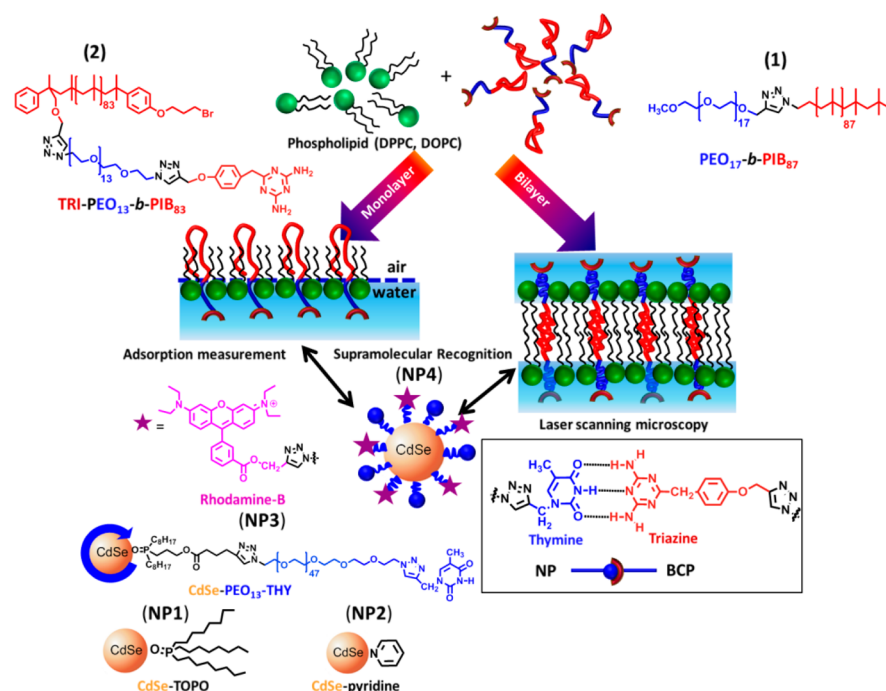


**Figure 1.** Concept for studying selective recognition via supramolecular hydrogen bond formation (see inset) between thymine-functionalized CdSe-NPs (NP3 and NP4) and triazine-functionalized hybrid lipid/BCP mono- and bilayer membranes, composed of either DPPC or DOPC in mixture with BCP 2 and/or BCP 1. NP1 and NP2 represent the chemical structure of the presteps in synthesizing THY-covered NP3 or NP4 via ligand exchange.

and bilayer membranes,<sup>24–26</sup> the ability of methyl- $\beta$ -CD to remove cholesterol and/or phospholipids with high efficiency was demonstrated, also explaining their toxicity (membrane rupture) in cellular systems.

Significantly more complex structures with highly specific and selective interactions were formed when mixed monolayers were used, still allowing to selectively recognize soluble analytes with the exactly matching hydrogen bonding pattern e.g., the recognition of flavine–adenine dinucleotide by mixed thymine/guanidine amphiphiles at the air/water interface<sup>27–29</sup> or the recognition of a dipeptide by a mixed guanidinium/amide monolayer.<sup>30,31</sup>

The strength of molecular recognition at the air/water interface can be significantly enhanced, which also leads to an increase in the association constant when compared to that of the respective interaction in bulk or in aqueous solution.<sup>18,32–36</sup> Additionally, multivalent molecular recognition at the air/water interface has been demonstrated in order to mimic the functional units of biological molecules like enzymes, proteins, and antibodies.<sup>9,29,37</sup> We<sup>38,39</sup> and others<sup>40–43</sup> have recently studied hybrid vesicles and monolayers as a result of blending natural lipids with synthetic polymer molecules forming hybrid membranes.<sup>44–49</sup> Depending on the composition and choice of lipids/polymers, either phase-segregated or homogeneously mixed membrane surfaces were observed.<sup>38,45,46,48</sup> The formation of biocompatible hybrid DPPC/PEO<sub>17</sub>-b-PIB<sub>87</sub> (BCP 1) bilayer membranes reported in our group<sup>38</sup> showed that their surface morphologies can be controlled by the lipid/BCP 1 mixing ratio (see Figure 1). Thus, GUVs prepared from mixtures with 0 to 14 mol % of BCP 1 showed a multifaceted vesicular surface typical for the gel phase behavior of DPPC liposomes, whereas GUVs from mixtures above 14 mol % of BCP 1 featured a completely closed membrane and a uniformly smooth surface. Furthermore, it was demonstrated that the

composition of hybrid lipid/block copolymer membranes composed of BCP 1 clearly influences the biological recognition between a membrane incorporated receptor molecule (ganglioside) and a water-soluble protein (cholera toxin).<sup>44</sup>

In this paper, we investigated the supramolecular recognition between an amphiphilic BCP 2 in mixtures with a lipid (DPPC or DOPC) and a multivalent nanoparticle (NP3 and NP4), as illustrated in Figure 1. To address a specific supramolecular interaction, the amphiphilic BCP 2 (TRI-PEO<sub>13</sub>-b-PIB<sub>83</sub>) was engineered to carry a 2,4-diaminotriazine (TRI) moiety on the hydrophilic PEO chain, thereby positioning the triaminotriazine at the vesicular surface of the mixed lipid/polymer membrane. In turn, supramolecular recognition between a rhodamine B-labeled thymine-functionalized CdSe nanoparticle (NP4) and a triazine (TRI)-functionalized BCP 2 was investigated using laser scanning microscopy and adsorption monolayer measurement.

## EXPERIMENTAL SECTION

**Materials. Solvent and Reagents.** All chemicals were purchased from Sigma-Aldrich (Schnelldorf, Germany) and were used as received unless otherwise stated. All solvents used for the synthesis of the diblock copolymer, and work-up procedures were distilled prior to use. Toluene and tetrahydrofuran (THF) were predried over potassium hydroxide for several days, refluxed over sodium/benzophenone, and freshly distilled under an argon atmosphere. The diblock copolymer PEO<sub>17</sub>-b-PIB<sub>87</sub> (BCP 1) ( $M_{n(NMR)} = 5900$  g/mol determined by <sup>1</sup>H NMR) with a polydispersity (PDI  $\leq 1.2$ ), used in this study, was synthesized in our laboratories via a combination of a living carbocationic polymerization method and the azide/alkyne “click” reaction, as reported previously.<sup>38</sup>

**Measurements. UV–vis Measurements.** UV–vis spectra were recorded using a PerkinElmer Lambda 18 UV–vis spectrometer.

Samples were dissolved in chloroform (HPLC-grade purchased from VWR Darmstadt Germany) in a concentration of 0.5 mg/mL.

**Thermogravimetric Analysis (TGA).** TGA was conducted on a Mettler Toledo (DSC-H22) instrument. The sample was heated in an aluminum oxide ( $\text{Al}_2\text{O}_3$ ) crucible, under a nitrogen atmosphere over a temperature range of 25–800 °C and a heating rate of 10 K min<sup>-1</sup>.

**Adsorption Measurements.** Adsorption experiments at the air/water interface were carried out at 20 °C on a circular Langmuir trough with a diameter of 3 cm, a depth of 1.39 cm, and a subphase volume of 10.25 mL (Riegler & Kirstein, Berlin, Germany). The adsorption experiments were conducted starting with different initial surface pressures of the mixtures containing the lipid and the hydrogen-bonded block copolymer TRI-PEO<sub>13</sub>-*b*-PIB<sub>83</sub> (2) or PEO<sub>17</sub>-*b*-PIB<sub>87</sub> BCP (1) devoid of hydrogen bonds for control experiments (with 20 mol % of diblock copolymer). For preparation of the mixed monolayers, a defined amount of the lipid/polymer mixture in HPLC-grade  $\text{CHCl}_3$  was spread with a digital Hamilton microsyringe onto the water subphase of Millipore quality (total organic carbon <5 ppm; conductivity <0.055  $\mu\text{S}/\text{cm}$ ). After waiting for 20 min for complete solvent evaporation and uniform dispersion of the monolayer molecules at the air/water interface, 20  $\mu\text{L}$  of the thymine-functionalized water-soluble hydrophilic CdSe nanoparticles (NP3) (5 mg/mL) was injected into the subphase below the monolayers through a channel located at the bottom of the Langmuir trough. To ensure a homogeneous bulk concentration of NPs in the subphase and in order to avoid large perturbations at the air/water interface, the subphase was gently stirred with a small rolling sphere. The changes in surface pressure ( $\text{mN m}^{-1}$ ) at the air/water interface caused by the supramolecular recognition between NP3 and the hydrogen-bonded BCP 2 were monitored as a function of time (seconds) by measuring the initial and final surface pressure using a filter paper as Wilhelmy plate.

**Dynamic Light Scattering.** DLS measurements were performed in chloroform solutions of the NPs after dilution by  $\sim 1/50$  with pure solvent on a Viscotek 802 using OmniSIZE software.

**Hybrid GUV Formation.** The formation of lipid (DPPC or DOPC)/TRI-PEO<sub>13</sub>-*b*-PIB<sub>83</sub> BCP (2) hybrid GUVs was achieved as described previously.<sup>38</sup> Water, which was used for the study, was purified via a passage through a filtering system by the Purelab Option system (ELGA Ltd., Celle, Germany), yielding ultrapure water. The lipid/polymer mixtures were prepared in chloroform (HPLC grade, Sigma-Aldrich, Schnellendorf, Germany), dried under a continuous  $\text{N}_2$  stream, and finally dissolved in a defined solvent volume reaching a total concentration of 10 mg/mL. The final mixtures were used to generate a homogeneous thin film on optically transparent indium–tin oxide (ITO)-coated coverslips (electrodes) via a spin-coating method. Laser scanning microscopy observations were facilitated by adding the fluorescent membrane dye DiDC<sub>18</sub> at an amount of 0.1 mol % to all lipid/polymer mixtures.

**Supramolecular Recognition Studies with Rhodamine B-Labeled Water-Soluble CdSe NP (NP4).** All supramolecular recognition studies between NP4 and hybrid GUVs consisting either of DPPC or DOPC with incorporated TRI-PEO<sub>13</sub>-*b*-PIB<sub>83</sub> BCP 2 and/or the PEO<sub>17</sub>-*b*-PIB<sub>87</sub> BCP 1 were conducted at room temperature (20 °C). After the electroformation process, the prepared GUVs with incorporated BCP molecules were first cooled down to room temperature, monitored by laser scanning microscopy revealing changes in their membrane morphologies, and afterward incubated with an aqueous solution of nanoparticles (NP4). Using a microsyringe, 50  $\mu\text{L}$  (3 mg/mL) of the water-soluble CdSe nanoparticle solution was injected into the flow chamber which contains the freshly prepared vesicles. The recognition process was thereafter monitored by laser scanning microscopy. All recognition studies were performed using fluorescently labeled NP (NP4) (excited at 561 nm, green color).

**Giant Vesicle Analysis by Confocal Laser Scanning Microscopy (cLSM).** Confocal microscopy images were obtained on a commercially available confocal-laser scanning microscope (Leica TCS SP2 DM IRE2, Germany) using a HCX PL APO 63 $\times$  1.2 water immersion objective. The thymine-functionalized water-soluble NPs which were further fluorescently labeled with rhodamine-B (NP4) were excited

with a DPSS laser at 561 nm. All GUVs were labeled with the lipid dye DiDC<sub>18</sub> (excited at 633 nm, red colored). Imaging studies and monitoring the supramolecular recognition between the NP4 and BCP 2 in hybrid GUVs were performed after cooling to room temperature (20 °C). Single scans were recorded with 8 $\times$  or 16 $\times$  line average. Z-stack acquisitions were performed from bottom to top. Images were processed with the software provided by Leica.

**Synthesis.** In order to engineer an amphiphilic molecule bearing an hydrogen bonding moiety, TRI-PEO<sub>13</sub>-*b*-PIB<sub>83</sub> BCP (2) was synthesized by a 2-fold stepwise click reaction similar to an earlier published method (for details on the synthetic pathway of the final block copolymer (2) see Scheme S1 and synthesis in the Supporting Information).<sup>50</sup> Trioctylphosphine oxide (TOPO)-covered CdSe-NPs (NP1) were synthesized by the conventional hot injection method according to ref 51. Ligand exchange of the relatively stable passivating TOPO on the CdSe nanoparticle surface with an appropriate polymer was conducted according to the literature,<sup>52,53</sup> yielding the PEO<sub>47</sub>-thymine (THY)-functionalized CdSe nanoparticle (NP3) (see Scheme S3). The TOPO ligand in NP1 was replaced with a relatively weak pyridine ligand in order to facilitate the ligand exchange and subsequently treating the pyridine-covered CdSe nanoparticles NP2 (50 mg) with  $\alpha$ -phosphine oxide- $\gamma$ -thymine telechelic poly(ethylene oxide) PO-PEO<sub>47</sub>-THY (see details on the synthetic pathway of compound 12a in Scheme S2) ( $M_{\text{n(GPC)}} = 2100$  g/mol;  $M_{\text{w}}/M_{\text{n}} = 1.3$ ) (179 mg). The nanoparticles were dissolved in 10 mL of freshly distilled anhydrous toluene; then the resulting mixture was stirred for 48 h at 70 °C. Toluene was evaporated under reduced pressure, and the PO-PEO<sub>47</sub>-THY-covered NPs (NP3) were precipitated three times in 20 mL of hexane followed by centrifugation to separate the free unbound polymer ligand (12a) from the PEO<sub>47</sub>-covered nanoparticles. The grafting density of the final NP3 was determined via TGA to be 0.7 chain/nm<sup>2</sup>.

**Synthesis of Polymer-Covered Rhodamine B-Labeled CdSe Nanoparticles (NP4).** To enable the observation with fluorescence microscopy of the hydrophilic CdSe NPs (NP3), they were fluorescently labeled with rhodamine B as follows (see also Scheme S3): a 50 to 50 mol % mixture of ligands 12a and 12b (see details on synthetic pathway of compound 12b in the Supporting Information) was dissolved in toluene and subsequently added to 50 mg of NP2. The mixture was heated at 60 °C for 48 h. Toluene was evaporated under reduced pressure, and the rhodamine-B labeled NPs (NP4) were precipitated three times in 20 mL of hexane followed by centrifugation to separate the free polymer ligand from the polymer-covered nanoparticles.

## RESULTS AND DISCUSSION

In order to investigate the supramolecular recognition between the multivalent THY-functionalized nanoparticles (NP3 and NP4) and mixed lipid/polymer membranes composed of DPPC or DOPC as lipid component in mixture with TRI-PEO<sub>13</sub>-*b*-PIB<sub>83</sub> BCP (2) or PEO<sub>17</sub>-*b*-PIB<sub>87</sub> BCP (1) as polymer component, hydrophilic CdSe nanoparticles (sized  $\sim 2$  nm) with grafted PEO<sub>47</sub>-THY chains on their surface were synthesized via a ligand exchange approach as reported earlier in our group.<sup>46</sup> NP4 were further labeled with rhodamine B to enhance its visualization by laser scanning microscopy to monitor the recognition process. As it is known from literature that unsaturated lipids like DOPC ( $T_{\text{m}} = -20$  °C) are more fluid at room temperature than saturated lipids like DPPC ( $T_{\text{m}} = 41.6$  °C),<sup>54</sup> we therefore investigated the role of membrane fluidity in the removal of membrane components by selective recognition and binding of water-soluble molecules, similar to what has been reported for cholesterol/cyclodextrin interactions at mono- and bilayer membranes.<sup>15</sup>

**Interaction of NP4 with Binary and Ternary DPPC/Polymer Mixtures.** We previously have demonstrated the formation of a biocompatible hybrid bilayer membranes



composed of a synthesized amphiphilic PEO<sub>17</sub>-*b*-PIB<sub>87</sub> BCP (1) and a natural lipid (DPPC).<sup>38</sup> To introduce a supramolecular recognition unit into our hybrid lipid/polymer system, we have synthesized an amphiphilic block copolymer TRI-PEO<sub>13</sub>-*b*-PIB<sub>83</sub> (2) bearing a hydrogen bonding moiety (triazine (TRI)) on the PEO chain, but comparable to the PEO<sub>17</sub>-*b*-PIB<sub>87</sub> BCP (1) in its hydrophobic/hydrophilic chain length ratio (for details see Supporting Information). We therefore expected the incorporation of this TRI-PEO<sub>13</sub>-*b*-PIB<sub>83</sub> BCP (2) into the lipid bilayer, thus functionalizing the GUV surfaces with moieties available to enable supramolecular recognition at the bilayer/water interface. Hybrid GUVs were prepared from a mixture of DPPC and 16 mol % of pure TRI-PEO<sub>13</sub>-*b*-PIB<sub>83</sub> BCP (2), featuring a completely round and smooth vesicle surface stable when monitored over several hours. The results in Figure 2A,B

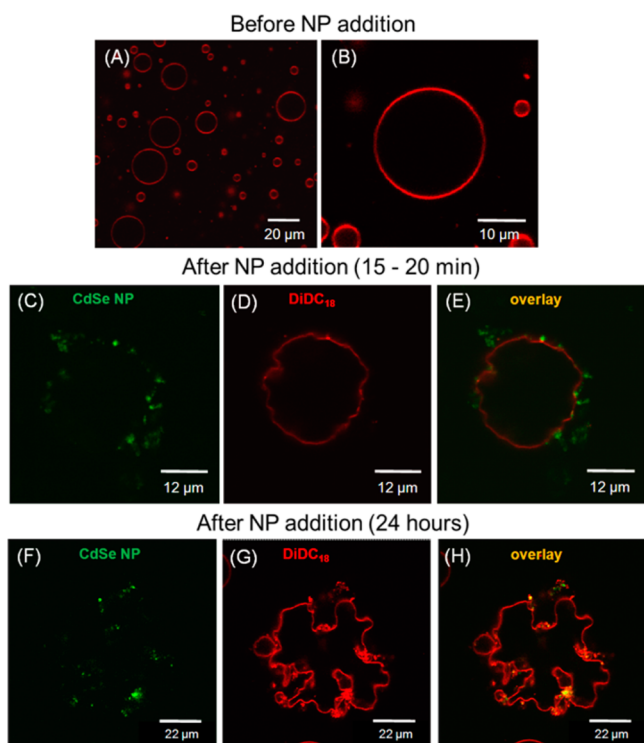


**Figure 2.** Confocal microscopy images of freshly prepared hybrid GUVs composed of DPPC and 16 mol % TRI-PEO<sub>13</sub>-*b*-PIB<sub>83</sub> BCP (2) showing the faceting effect of the vesicles upon addition of NP4. (A, B) Overview and a single GUV image of hybrid GUVs, which were obtained from DPPC and 16 mol % TRI-PEO<sub>13</sub>-*b*-PIB<sub>83</sub> BCP (2) labeled with DiDC<sub>18</sub>. (C, F) Fluorescence of the rhodamine B-labeled PEO<sub>47</sub>-thymine-covered CdSe NP (NP4) (green; excited at 561 nm) showing their binding to the mixed GUV. (D, G) A single-faceted GUV after 15 min and 24 h of NP4 addition (red; excited at 633 nm). (E, H) Overlay images showing the fluorescence of (NP4) as they bind to the GUVs after 15 min and 24 h of NP4 addition.

are in accordance with previous investigation using PEO<sub>17</sub>-*b*-PIB<sub>87</sub> BCP (1) to prepare hybrid GUVs,<sup>38</sup> indicating no phase separation with respect to the resolution limit of the microscope (200–300 nm). Subsequently, a solution of NP4 (3 mg/mL) was added to selectively recognize the triazine moiety of TRI-PEO<sub>13</sub>-*b*-PIB<sub>83</sub> BCP (2) in the hybrid GUVs. In the initial 5–10 min after NP addition into the freshly prepared GUV suspension, the thymine-functionalized nanoparticles NP4 recognize the triazine moiety of the BCP 2 within the mixed membrane, which effects the binding of the NP4 to the

membrane surface visible by increased fluorescence intensity of the NPs at the vesicle surface (excited at  $\lambda_{\text{max}} = 561$  nm, rhodamine B) (Figure S9).

After 15–20 min of nanoparticle addition (see Figure 2C–E), faceting of the vesicle surface typical for pure DPPC or vesicles with less polymer content (<14 mol %) was observed. This effect could be explained as a result of the removal of the TRI-PEO<sub>13</sub>-*b*-PIB<sub>83</sub> BCP (2) from the mixed GUVs, thereby leaving the DPPC vesicles with reduced polymer content in their gel phase state (stable even after 24 h, Figure 2F–H).

As reported in literature,<sup>13</sup> the single association constant ( $K_a$ ) of thymine/triazine at the air/water interface was found to be  $2 \times 10^2 \text{ M}^{-1}$ . This single association between thymine/triazine can be significantly enhanced by the multivalency of the thymine-functionalized NP4 when they undergo supramolecular recognition with the triazine chain end of the membrane-incorporated BCP 2 molecules, leading to a much stronger interaction. Thus, a selective removal of the BCP 2 from the hybrid bilayer membrane can be explained, analogous to the reported selective removal of cholesterol from lipid membranes by cyclodextrin derivatives displaying a binding constant of  $\sim 1.7 \times 10^4 \text{ M}^{-1}$ .<sup>55</sup>

To exclude unspecific destruction of the vesicle surface by the added nanoparticles,<sup>56,57</sup> a control experiment was conducted where GUVs were prepared using a mixture of DPPC and 16 mol % of PEO<sub>17</sub>-*b*-PIB<sub>87</sub> BCP (1) devoid of any hydrogen-bonding moieties; in contrast, the hybrid vesicles remained completely round with a smooth surface even after 24 h of NP4 addition (see Figure 3). The observed stability of the

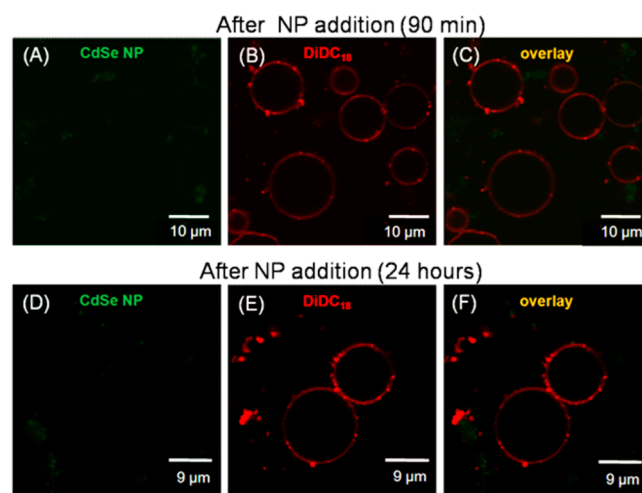


**Figure 3.** Confocal microscopy images of freshly prepared hybrid GUVs composed of DPPC and 16 mol % PEO<sub>17</sub>-*b*-PIB<sub>87</sub> BCP (1). (A, D) Fluorescence of the rhodamine B-labeled PEO<sub>47</sub>-thymine-covered CdSe NP (NP4) (green; excited at 561 nm). (B, E) Single-faceted GUVs after 15 min and 24 h of NP4 addition (red; excited at 633 nm). (C, F) Overlay images showing the fluorescence of (NP4) compared to DiDC<sub>18</sub> membrane dye.

hybrid GUVs prepared from this mixture (16 mol % of BCP 1) shows that the previously observed vesicle faceting in the case of DPPC and 16 mol % of BCP 2 is not a result of unspecific vesicle destruction by the nanoparticles.

To investigate the ability of the TRI-PEO<sub>13</sub>-*b*-PIB<sub>83</sub> BCP (2) to form a phase-separated membrane morphology as reported for PEO<sub>17</sub>-*b*-PIB<sub>87</sub> BCP (1),<sup>38</sup> we prepared GUVs from DPPC and 24 mol % of TRI-PEO<sub>13</sub>-*b*-PIB<sub>83</sub> BCP (2). Unexpectedly,

in contrast to PEO<sub>17</sub>-*b*-PIB<sub>87</sub> BCP (1), the obtained vesicles featured a well-mixed membrane morphology. Addition of NP4 also induced vesicle facettation (data not shown). To further mimic biological receptor/ligand binding processes, we studied the selective recognition of BCP 2 by NP4 in hybrid GUVs from a more complex ternary mixture containing DPPC, 11 mol % of PEO<sub>17</sub>-*b*-PIB<sub>87</sub> BCP (1), and 5 mol % of TRI-PEO<sub>13</sub>-*b*-PIB<sub>83</sub> BCP (2). As these mixed GUVs now contain a total amount of 16 mol % of BCP (1 and 2) as mentioned earlier, they should display a completely closed membrane and a uniformly smooth surface. In Figure 4A,B, the obtained hybrid

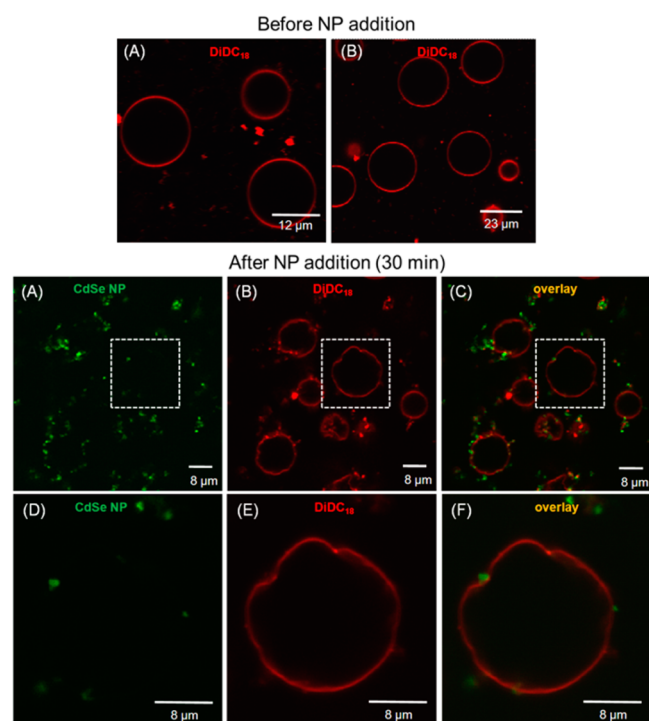


**Figure 4.** Confocal microscopy images of freshly prepared hybrid GUVs composed of DPPC with 11 mol % PEO<sub>17</sub>-*b*-PIB<sub>87</sub> BCP (1) and 5 mol % of TRI-PEO<sub>13</sub>-*b*-PIB<sub>83</sub> BCP (2). (A, B) An overview and a single GUV image of mixed hybrid GUVs. (C, F) Fluorescence of the rhodamine B-labeled PEO<sub>47</sub>-thymine-covered CdSe NP (NP4) (green; excited at 561 nm) showing their binding to the mixed GUV. (D, G) Single-faceted GUVs after 30 min of NP4 addition (red; excited at 633 nm). (E, H) Overlay images showing the fluorescence of the (NP4) after 30 min of NP addition (green; excited at 561 nm) compared to DiDC<sub>18</sub>.

GUVs from the now ternary mixture indeed showed a completely closed membrane and a uniformly smooth surface, stable over several hours. Adding NP4 to the solution of the hybrid GUVs, the hybrid vesicles again became faceted after 20–30 min of the NP addition as shown in Figure 4G,H. As a result of the supramolecular interaction between the thymine-functionalized nanoparticles and the triazine of the BCP 2, followed by the selective removal of BCP 2 from the mixed membrane now leaving behind the PEO<sub>17</sub>-*b*-PIB<sub>87</sub> BCP (1) devoid of hydrogen bonds. As this remaining amount of BCP 1 is not sufficient to prevent the formation of extended areas of gel phase in DPPC, the facetation was observed, as explained in the literature.<sup>38</sup>

**Interaction of NP4 with Binary and Ternary DOPC/Polymer Mixtures.** As known from the literature, unsaturated lipids like DOPC ( $T_m = -20$  °C) are more fluid at room

temperature in comparison to saturated lipids like DPPC ( $T_m = 41.6$  °C).<sup>54</sup> We therefore investigated the supramolecular recognition between the triazine-functionalized BCP 2 and the multivalent NP4 in a more fluidic system (using DOPC), having in mind that DOPC/polymer hybrid vesicles might show a different behavior compared to the facetation observed in DPPC membranes.

GUVs were first prepared from pure DOPC, which is known to feature a completely closed membrane and a uniformly smooth surface in concordance to the literature.<sup>58</sup> Our prepared DOPC GUVs featured a completely closed membrane and a uniformly smooth surface separated from each other and stable when monitored over several hours (see Figure 5A).

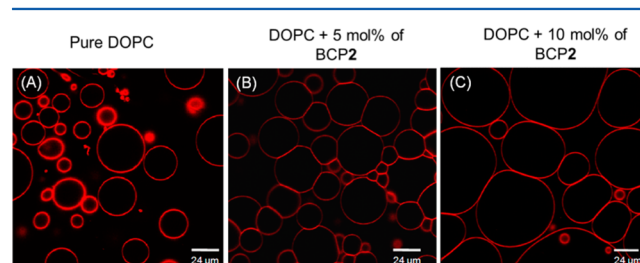


**Figure 5.** Confocal microscopy images of freshly prepared hybrid GUVs: (A) pure DOPC, (B) mixture of DOPC and 5 mol % of TRI-PEO<sub>13</sub>-*b*-PIB<sub>83</sub> BCP (2), and (C) mixtures of DOPC and 10 mol % of TRI-PEO<sub>13</sub>-*b*-PIB<sub>83</sub> BCP (2) showing mixed GUVs which are connected to each other.

The formed hybrid GUVs observed from mixtures of DOPC with either 5 or 10 mol % of TRI-PEO<sub>13</sub>-*b*-PIB<sub>83</sub> BCP (2) displayed the formation of contact areas between the vesicles, as shown in Figure 5B,C. These contact areas could be a result of the hydrogen bond interaction between the triazine molecules within the hybrid DOPC/BCP membranes, due to the now increased lateral fluidity as compared to hybrid GUVs from DPPC (rigid bilayers at RT) and BCPs. By addition of NP4 to the freshly prepared suspension of hybrid GUVs containing either 5 or 10 mol % BCP 2 (10 mol % case shown in Figure 6), NPs were specifically attracted to the edges of the formed contact areas between the hybrid GUVs where the polymers are concentrated by forming the intervesicular hydrogen bonds (see overview in Figure 6A–C). Recognition and subsequent binding of NP4 to the triazine-functionalized vesicle surfaces lead to reduction of these intervesicular contact areas (see magnified membrane contact regions in Figure 6E,F).

The removal of the TRI-PEO<sub>13</sub>-*b*-PIB<sub>83</sub> BCP (2) was confirmed by destruction of all hybrid vesicles within minutes (most of all within 30 min) after addition of NP4 (see also Figure S10 showing a time series and Figures S11 and S12 demonstrating microscopy images of destructed GUVs). In general, we expected that the more fluid DOPC membrane compensates for polymer extraction by the NPs better rather than DPPC (highly rigid membranes at RT), but the experimental results clearly show that in case of fluid membranes all hybrid GUVs were destroyed by the fast polymer extraction (within minutes). This destruction of giant vesicles might be explained by the bending rigidity concept<sup>59</sup> of fluid membranes (DOPC), allowing high membrane curvatures of the lipid bilayer. Fluid membranes have much smaller bending rigidities (i.e., higher flexibilities)<sup>60</sup> compared to gel-phase membranes of DPPC (high bending rigidity)—thus

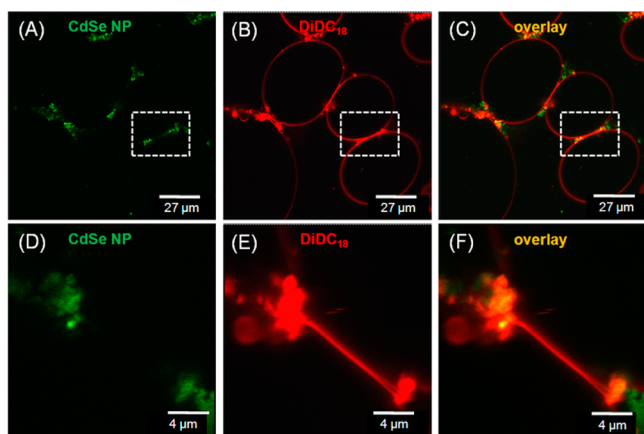


**Figure 6.** Confocal microscopy images of hybrid GUVs prepared from mixtures of DOPC and 10 mol % of TRI-PEO<sub>13</sub>-*b*-PIB<sub>83</sub> BCP (2): (A–C) the specific attraction of NP4 at the edges of the observed contact areas (i.e., BCP 2-rich areas of the vesicular membrane); (D–F) the magnified area of the single GUVs as indicated in (A–C); the specific recognition of the thymine-functionalized NP4 at the BCP 2-rich regions of the polymer can be observed.

during BCP 2 extraction from the lipid bilayers, many defects in the membrane were formed in case of fluid DOPC, resulting in membrane fragments (nanometer range), which self-close to small unilamellar vesicles (highly curved membrane). As consequence, the initial hybrid DOPC/BCP GUVs vanished, and the formed small DOPC-rich vesicles were not detected by LSM due to the resolution limit of the microscope ( $\sim 200$ – $300$  nm).

In a control experiment, GUVs were prepared using a mixture of DOPC with 10 or 15 mol % of BCP 1 devoid of hydrogen-bonding moieties. The mixed GUVs also exhibited a completely round and smooth surface without the formation of contact areas when monitored for several hours. Addition of NP4 did not have any significant effect on the mixed GUVs in the first hours of monitoring (data not shown), which is remarkably different from the result observed in the mixed GUVs with BCP 2 having hydrogen-bonding moieties. After 24 h, we observed that some of the vesicles from DPPC and BCP 1 were still stable (round and smooth shape), whereas some were destroyed. On the basis of the observed removal of the triazine-functionalized polymers (2) from the mixed GUVs in the earlier discussed experiments, we decided to prepare GUVs from a ternary mixtures of DOPC with 15 mol % of BCP 1 and 5 mol % of BCP 2, keeping in mind that if the 5 mol % of TRI-PEO<sub>13</sub>-*b*-PIB<sub>83</sub> BCP (2) is removed after NP4 addition, the remaining 15 mol % of PEO<sub>17</sub>-*b*-PIB<sub>87</sub> BCP (1) might be sufficient to maintain stable vesicles. Thus, GUVs prepared from mixtures of DOPC containing 15 mol % of BCP 1 and 5 mol % of BCP 2 also featured a completely closed membrane and a uniformly smooth surface (see Figure S13A). These vesicles were still visible after 60 min of NP4 addition to the freshly prepared hybrid GUVs (see Figure S13B–D). The observed vesicles were stable as a consequence of the remaining 15 mol % of BCP 1 in the mixed membrane which thus improved significantly the stability of DOPC GUVs during the selective removal of BCP 2.

To further investigate the effect of NP4 on pure DOPC vesicles devoid of any hydrogen bonds, NP4 was added to freshly prepared DOPC vesicles, which showed no destruction of the vesicles, when monitored over several hours (see Figure S14).

These observations in contrast to hybrid DOPC/BCP GUVs prove that the observed vesicle destruction in case of DOPC/BCP 2 vesicles was induced by the selective removal of the triazine-functionalized polymer molecules from the hybrid membrane when the multivalent NP4 was added.

**Monolayer Adsorption Experiments of Hydrophilic CdSe NP (NP3) with Binary Lipid/Polymer Mixtures.** In order to better understand the nature of the supramolecular interaction observed in the bilayer experiment resulting to a selective removal of BCP 2 due to the recognition and binding by NP4, we have chosen to study the supramolecular interaction by monolayer adsorption measurements. Adsorption experiments were earlier conducted in our laboratory<sup>46</sup> on mixed DPPC/BCP 1 monolayers with hydrophilic PEO-covered CdSe NPs at the air/water interface. The high affinity of the PEO-functionalized NPs toward the hydrophilic portion of the BCP molecules was clearly seen by comparing the changes in surface pressure of a pure lipid and hybrid monolayer with increasing polymer content, assuming that the submerged PEO chains of the BCPs might serve as a barrier for the PEO-covered NPs (preferred interactions), preventing the NPs from approaching the air/water interface.

Therefore, we investigated the supramolecular recognition between the PEO<sub>47</sub>-thymine-functionalized nanoparticles (NP3) and hybrid monolayers from mixture of lipid (DPPC or DOPC) with BCP 2 at the air/water interface. In adsorption monolayer measurements, the lipid/polymer mixture is first spread on the subphase at the air/water interface, followed by injection of the nanoparticles into the subphase after reaching a stable monolayer (constant surface pressure).

Changes in the surface pressure were measured as a function of time after injecting the NP3 into the subphase, as shown in Figures 7 and 8. From the adsorption measurement

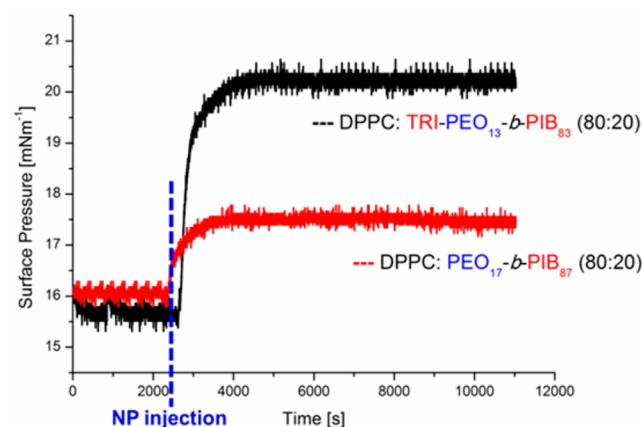


**Figure 7.** Time-dependent Langmuir adsorption isotherms of hybrid monolayers after injection of NP3 into the subphase below the monolayer, which is composed of a binary mixtures of DPPC (80 mol %)/TRI-PEO<sub>13</sub>-*b*-PIB<sub>83</sub> BCP (2) (20 mol %) (black curve) or DPPC/PEO<sub>17</sub>-*b*-PIB<sub>87</sub> BCP (1) (red curve), at 20 °C with an initial surface pressures of 16 mN m<sup>−1</sup>.

immediately after injecting the NP3 (time of injection marked in blue in Figure 7) the surface pressure starts to increase (as a result of the supramolecular interaction of NPs with BCP 2 at the air/water interface and/or due to the surface activity of the NPs) until an equilibrium value  $\pi_{eq}$  is reached, where a significant increase in the surface pressure could no longer be observed. In the case of DPPC/TRI-PEO<sub>13</sub>-*b*-PIB<sub>83</sub> mixtures



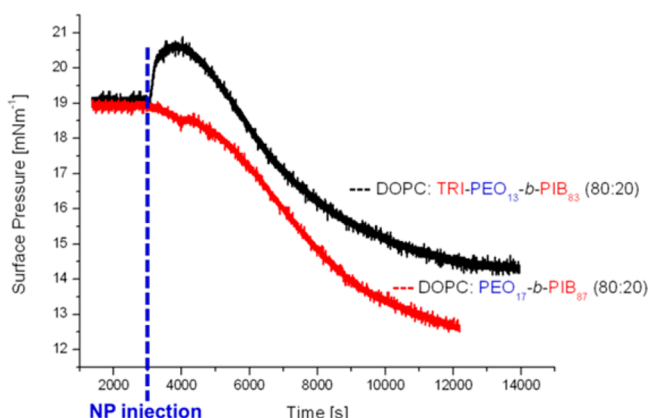


**Figure 8.** Time-dependent Langmuir adsorption isotherms of hybrid monolayers after injection of NP3 into the subphase below the monolayer, which is composed of either DOPC/TRI-PEO<sub>13</sub>-*b*-PIB<sub>83</sub> (black curve) or DPPC/PEO<sub>17</sub>-*b*-PIB<sub>87</sub> BCP (red curve), at 20 °C with an initial surface pressures of 19 mN m<sup>-1</sup>.

higher changes in the surface pressure  $\Delta\pi$  ( $\Delta\pi = \pi_{eq} - \pi_0$ ) indicate that the multivalent PEO<sub>47</sub>-thymine-covered NPs can recognize the triazine moiety of BCP 2 at the air/water interface. Comparing the mixture of DPPC/PEO<sub>17</sub>-*b*-PIB<sub>87</sub> (red curve) with DPPC/TRI-PEO<sub>13</sub>-*b*-PIB<sub>83</sub> (black curve) in Figure 7, it could be clearly seen that the supramolecular recognition between NP3 and BCP 2 leads to a significant higher increase in surface pressure as compared to the nonspecifically interacting DPPC/BCP 1 mixtures.

The higher surface pressure change that was observed in the DPPC/BCP 2 mixture is a result of the rapid adsorption of the NPs onto the hydrophilic portion of the monolayer supported by the hydrogen bond interactions between thymine and triazine moieties. Additionally as now the C<sub>8</sub>H<sub>17</sub> chains attached to the NP3 (see chemical structure in Scheme S3) are close to the air/water interface, the strong increase in surface pressure can be the result of the insertion of the C<sub>8</sub>H<sub>17</sub> chains into the hydrophobic portion of the hybrid monolayer. On the basis of this argument, we suggest that the much higher increase in surface pressure in case of the triazine-functionalized monolayer (DPPC/BCP 2) compared to the DPPC/BCP 1 is justified by the specific supramolecular recognition between NP3 and BCP 2. Thus, the particles closer to the air/water interface enable a much higher incorporation of the hydrophobic C<sub>8</sub>H<sub>17</sub> chains rather than in case of the nonspecifically interacting DPPC/BCP 1 monolayer, where the insertion of the C<sub>8</sub>H<sub>17</sub> chains is just a statistical event.

To understand the role of fluidity as earlier explained in the case of bilayer investigations, we studied the interaction of the water-soluble thymine-functionalized NPs (NP3) with hybrid monolayer from DOPC and BCP 2 or BCP 1. After injection of the NPs into the subphase (see blue mark in Figure 8), an initial rise in the surface pressure was only noticed in case of the triazine-functionalized monolayer (DOPC/BCP 2), demonstrating the specific supramolecular recognition between the nanoparticles and BCP 2 molecules. The initial increase in surface pressure was followed by the drastic drop of the surface pressure, which might be explained by the selective removal of the polymer component (BCP 2) from the mixed monolayer into the subphase (see black curve in Figure 8). This result is consistent with those observed in the bilayer measurement, where the mixed GUVs prepared from a mixture of DOPC and

BCP 2 were completely destroyed after addition of NP4 (within minutes). In case of the nonspecifically interacting monolayer (DOPC/BCP 1) without any hydrogen-bonding moiety, a sudden decrease in surface pressure was observed after injecting NP3 into the subphase. This drastic decrease in surface pressure might be caused by the diffusion of the nanoparticles to the air/water interface due to their surface activity, thereby inducing the collapse of the hybrid monolayer (see red curve in Figure 8) as shown by the strong drop from 19 mN/m to less than 13 mN/m within 150 min.

## CONCLUSION

The basic idea of this investigation concerned the recognition between a mixed membrane (lipid/amphiphilic block copolymer (BCP 1 and/or BCP 2)) and a multivalent nanoparticle (NP3 or NP4), with one membrane component (BCP 2) being able to recognize a specific hydrogen bond on the NP surface. In detail, the supramolecular recognition of a triple hydrogen bond (TRI/THY) between the amphiphilic BCP 2 in mixture with either a liquid crystalline (DPPC) or a fluid (DOPC) lipid and a multivalent nanoparticle (NP3 and NP4) was chosen to effect a specific (multivalent) interaction between one membrane component and the nanoparticle. In a first step, the preparation of the amphiphilic block copolymer TRI-PEO<sub>13</sub>-*b*-PIB<sub>83</sub> (2) was accomplished carrying a 2,4-diaminotriazine (TRI) moiety on the hydrophilic PEO chain, thereby positioning the diaminotriazine at the vesicular surface of the mixed lipid/polymer membrane. In turn, supramolecular recognition between a rhodamine B-labeled thymine-functionalized CdSe nanoparticle (NP4) and a triazine-functionalized BCP (2) was investigated using laser scanning microscopy and adsorption monolayer measurements.

Using hybrid GUVs as model bilayer membrane, NPs with surface bound THY moieties (NP3) interacted specifically with a mixture of DPPC and 16 mol % of pure TRI-PEO<sub>13</sub>-*b*-PIB<sub>83</sub> BCP (2), first recognizing the triazine moiety of BCP 2 within the mixed membrane, followed by removing the polymer component (BCP 2) from the mixed vesicular membrane, thus leaving the DPPC GUVs with a now reduced polymer content in their respective gel phase state (stable even after 24 h). Several experiments (also in ternary mixture from DPPC/BCP 1/BCP 2) proved the selectivity of the interaction and the selective removal of the interacting BCP 2. Exchanging DPPC with DOPC as the now fluid lipid component at room temperature, GUVs fabricated from mixtures of DOPC/BCP 2 indicated a selective interaction between the hydrophilic PEO<sub>47</sub>-THY-functionalized CdSe-NPs (NP4) and BCP 2, again leading to a selective removal of the polymer component, which finally results into destruction of the giant vesicles via membrane rupture. The differences in bending rigidities of fluid DOPC membranes (highly flexible) in contrast to gel-phase membranes of DPPC (high bending rigidity) lead in the case of hybrid DOPC/BCP 2 membranes to the destruction of the GUVs into small vesicles, whereas the selective removal of BCP 2 from rigid DPPC membranes results in the formation of highly faceted giant vesicles as consequence of reducing the defects in the membrane obtained during the polymer extraction.

Adsorption experiments in mixed monolayers fabricated from DPPC/BCP 2 revealed that hydrophilic THY-functionalized NPs can specifically recognize the triazine-functionalized BCP 2 at the air/water interface, inducing significantly higher changes



in surface pressure when compared to a monolayer of the nonspecifically interacting DPPC/PEO<sub>17</sub>-*b*-PIB<sub>87</sub> mixture.

In summary, the presented method allows to specifically address recognition between membrane components and externally added nanoparticles via a relatively simple (supramolecular) interaction. Surprisingly, the binding efficiency of the in water weak THY/TRI interaction is sufficient to selectively remove one membrane component from the mixed mono- or bilayer membrane. Similar to experiments showing the selective cholesterol removal by cyclodextrins, the presented investigation enables to effect e.g. pore formation, selective vesicle disintegration, or the specific binding of nanoparticles to membrane receptors. The here demonstrated methodology is applicable to a large number of receptor molecules of similar or even stronger association constants between receptor and ligand. We thus do hope that this basic investigation can spur e.g. the selective capturing and detection of cancer cells via similar principles.

## ■ ASSOCIATED CONTENT

### ■ Supporting Information

Details on synthetic pathways of the final compounds BCP 2, polymer ligands 12a/12b and final NP3/NP4, Scheme S1; synthesis of the amphiphilic BCP TRI-PEO<sub>13</sub>-*b*-PIB<sub>83</sub> (2), Scheme S2; synthesis of the  $\alpha$ -PO-telechelic PEO<sub>47</sub> ligands (12a ( $\omega$ -THY) and 12b (rhodamine)), Scheme S3; synthesis of hydrophilic water-soluble and rhodamine-B/THY labeled CdSe NPs, proton NMR spectra of compound 4 (Figure S1); MALDI-TOF spectra of compound 4 (Figure S2); FT-IR spectra of compound 4 (Figure S3); proton NMR spectra of compound 2 (Figure S4); MALDI-TOF spectra of compound 2 (Figure S5); IR spectra of compound 2 (Figure S6); proton NMR spectra of compound 12a (Figure S7); MALDI-TOF spectra of compound 12a (Figure S8); confocal microscopy images of freshly prepared hybrid GUVs from DPPC with 16 mol % TRI-PEO<sub>13</sub>-*b*-PIB<sub>83</sub> BCP (2) showing binding of NPs to the membrane in the first 5–10 min after NP addition (Figure S9); hybrid GUVs prepared from DOPC with 10 mol % of TRI-PEO<sub>13</sub>-*b*-PIB<sub>83</sub> BCP (2) showing the destruction of vesicles with time induced by NP addition (Figure S10); hybrid GUVs prepared from DOPC with 10 mol % of TRI-PEO<sub>13</sub>-*b*-PIB<sub>83</sub> BCP (2); panels A–C show the specific attraction of NP4 into the polymer-rich areas of the vesicles inducing membrane rupture (Figure S11); hybrid GUVs prepared from DOPC with 10 mol % of TRI-PEO<sub>13</sub>-*b*-PIB<sub>83</sub> BCP (2); panels A–C show an overview of destroyed vesicles and panels D–F a magnification of a single destroyed GUV (Figure S12); hybrid GUVs prepared from a ternary mixture of DOPC with 15 mol % of BCP 1 and 5 mol % of BCP 2; panel A shows an overview image of hybrid GUVs before NP addition, panels B–D an overview after 60 min of NP4 addition, and panels E–G an overview after 24 h (Figure S13); confocal microscopy images, GUVs prepared from pure DOPC showing stable GUVs after addition of NP4 (monitored over several hours) (Figure S14). This material is available free of charge via the Internet at <http://pubs.acs.org>.

## ■ AUTHOR INFORMATION

### Corresponding Author

\*E-mail: [wolfgang.binder@chemie.uni-halle.de](mailto:wolfgang.binder@chemie.uni-halle.de) (W.H.B.).

### Notes

The authors declare no competing financial interest.

## ■ ACKNOWLEDGMENTS

We acknowledge grant DFG BI 1337/6-1 and DFG BI 1337/6-2 (W.H.B.) and DFG KR 1714/4-2 (J.K.) within the Forschergruppe FOR-1145 (A.O., M.S. and R.S.) and grants DFG INST 271/249-1, INST 271/247-1, and INST 271/248-1 for financial support.

## ■ REFERENCES

- (1) Jiang, H.; Smith, B. D. Dynamic molecular recognition on the surface of vesicle membranes. *Chem. Commun.* **2006**, 1407–1409.
- (2) Leblanc, R. M. Molecular recognition at Langmuir monolayers. *Curr. Opin. Chem. Biol.* **2006**, *10*, 529–536.
- (3) Oshovsky, G. V.; Reinhoudt, D. N.; Verboom, W. Supramolecular chemistry in water. *Angew. Chem., Int. Ed.* **2007**, *46*, 2366–2393.
- (4) Voskuhl, J.; Ravoo, B. J. Molecular recognition of bilayer vesicles. *Chem. Soc. Rev.* **2009**, *38*, 495–505.
- (5) Uzun, O.; Sanyal, A.; Jeong, Y.; Rotello, V. M. Molecular recognition induced self-assembly of diblock copolymers: Microspheres to vesicles. *Macromol. Biosci.* **2010**, *10*, 481–487.
- (6) Binder, W.; Zirbs, R. Hydrogen Bonded Polymers. In *Advances in Polymer Science*; Binder, W. H., Ed.; Wiley: New York, 2007; pp 1–78.
- (7) Fan, E.; Van Arman, S. A.; Kincaid, S.; Hamilton, A. D. Molecular recognition: hydrogen-bonding receptors that function in highly competitive solvents. *J. Am. Chem. Soc.* **1993**, *115*, 369–370.
- (8) Kurihara, K.; Ohto, K.; Honda, Y.; Kunitake, T. Efficient, complementary binding of nucleic acid bases to diaminotriazine-functionalized monolayers on water. *J. Am. Chem. Soc.* **1991**, *113*, 5077–5079.
- (9) Sasaki, D. Y.; Kurihara, K.; Kunitake, T. Specific, multiple-point binding of ATP and AMP to a guanidinium-functionalized monolayer. *J. Am. Chem. Soc.* **1991**, *113*, 9685–9686.
- (10) Ariga, K.; Nakanishi, T.; Hill, J. P. A paradigm shift in the field of molecular recognition at the air–water interface: from static to dynamic. *Soft Matter* **2006**, *2*, 465–477.
- (11) Ariga, K.; Ito, H.; Hill, J. P.; Tsukube, H. Molecular recognition: from solution science to nano/materials technology. *Chem. Soc. Rev.* **2012**, *41*, 5800–5835.
- (12) Ariga, K.; Kunitake, T. Molecular recognition at air–water and related interfaces: Complementary hydrogen bonding and multisite interaction. *Acc. Chem. Res.* **1998**, *31*, 371–378.
- (13) Kawahara, T.; Kurihara, K.; Kunitake, T. Cooperative binding of adenine via complementary hydrogen bonding to an imide functionalized monolayer at the air–water interface. *Chem. Lett.* **1992**, *21*, 1839–1842.
- (14) Hasegawa, T.; Hatada, Y.; Nishijo, J.; Umemura, J.; Huo, Q.; Leblanc, R. M. Hydrogen bonding network formed between accumulated Langmuir–Blodgett films of barbituric acid and triaminotriazine derivatives. *J. Phys. Chem. B* **1999**, *103*, 7505–7513.
- (15) Kong, X.; Du, X. In situ IRRAS studies of molecular recognition of barbituric acid lipids to melamine at the air–water interface. *J. Phys. Chem. B* **2011**, *115*, 13191–13198.
- (16) Xin, Y.; Kong, X.; Zhang, X.; Lv, Z.; Du, X. Self-assembly and molecular recognition of adenine- and thymine-functionalized nucleolipids in the mixed monolayers and thymine-functionalized nucleolipids on aqueous melamine at the air–water interface. *Langmuir* **2012**, *28*, 11153–11163.
- (17) Oishi, Y.; Torii, Y.; Kato, T.; Kuramori, M.; Suehiro, K.; Ariga, K.; Taguchi, K.; Kamino, A.; Koyano, H.; Kunitake, T. Molecular patterning of a guanidinium/orotate mixed monolayer through molecular recognition with flavin adenine dinucleotide. *Langmuir* **1997**, *13*, 519–524.
- (18) Onda, M.; Yoshihara, K.; Koyano, H.; Ariga, K.; Kunitake, T. Molecular recognition of nucleotides by the guanidinium unit at the surface of aqueous micelles and bilayers. A comparison of microscopic and macroscopic interfaces. *J. Am. Chem. Soc.* **1996**, *118*, 8524–8530.
- (19) Duan, P.; Qin, L.; Liu, M. Langmuir–Blodgett films and chiroptical switch of an azobenzene-containing dendron regulated by

the in situ host–guest reaction at the air/water interface. *Langmuir* **2010**, *27*, 1326–1331.

(20) Sanchez, S.; Gunther, G.; Tricerri, M.; Gratton, E. Methyl- $\beta$ -cyclodextrins preferentially remove cholesterol from the liquid disordered phase in giant unilamellar vesicles. *J. Membr. Biol.* **2011**, *241*, 1–10.

(21) Taneva, S.; Ariga, K.; Okahata, Y.; Tagaki, W. Association between amphiphilic cyclodextrins and cholesterol in mixed insoluble monolayers at the air–water interface. *Langmuir* **1989**, *5*, 111–113.

(22) Ohvo, H.; Slotte, J. P. Cyclodextrin-mediated removal of sterols from monolayers: effects of sterol structure and phospholipids on desorption rate. *Biochemistry* **1996**, *35*, 8018–8024.

(23) Besenčar, M. P.; Bavdek, A.; Kladnik, A.; Maček, P.; Anderluh, G. Kinetics of cholesterol extraction from lipid membranes by methyl- $\beta$ -cyclodextrin-A surface plasmon resonance approach. *Biochim. Biophys. Acta, Biomembr.* **2008**, *1778*, 175–184.

(24) Veatch, S. L.; Polozov, I. V.; Gawrisch, K.; Keller, S. L. Liquid domains in vesicles investigated by NMR and fluorescence microscopy. *Biophys. J.* **2004**, *86*, 2910–2922.

(25) Mascetti, J.; Castano, S.; Cavagnat, D.; Desbat, B. Organization of  $\beta$ -cyclodextrin under pure cholesterol, DMPC, or DMPG and mixed cholesterol/phospholipid monolayers. *Langmuir* **2008**, *24*, 9616–9622.

(26) Veatch, S. L.; Keller, S. L. Separation of liquid phases in giant vesicles of ternary mixtures of phospholipids and cholesterol. *Biophys. J.* **2003**, *85*, 3074–3083.

(27) Ariga, K.; Kamino, A.; Koyano, H.; Kunitake, T. Recognition of aqueous flavin mononucleotide on the surface of binary monolayers of guanidinium and melamine amphiphiles. *J. Mater. Chem.* **1997**, *7*, 1155–1162.

(28) Taguchi, K.; Ariga, K.; Kunitake, T. Multi-site recognition of flavin adenine dinucleotide by mixed monolayers on water. *Chem. Lett.* **1995**, *24*, 701–702.

(29) Sasaki, D. Y.; Kurihara, K.; Kunitake, T. Self-assembled multifunctional receptors for nucleotides at the air–water interface. *J. Am. Chem. Soc.* **1992**, *114*, 10994–10995.

(30) Cha, X.; Ariga, K.; Kunitake, T. Molecular recognition of aqueous dipeptides at multiple hydrogen-bonding sites of mixed peptide monolayers. *J. Am. Chem. Soc.* **1996**, *118*, 9545–9551.

(31) Ariga, K.; Kamino, A.; Cha, X.; Kunitake, T. Multisite recognition of aqueous dipeptides by oligoglycine arrays mixed with guanidinium and other receptor units at the air–water interface. *Langmuir* **1999**, *15*, 3875–3885.

(32) Berndt, P.; Kurihara, K.; Kunitake, T. Adsorption of poly(styrenesulfonate) onto an ammonium monolayer on mica: a surface forces study. *Langmuir* **1992**, *8*, 2486–2490.

(33) Swairjo, M. A.; Seaton, B. A.; Roberts, M. F.; Roberts, M. F. Effect of vesicle composition and curvature on the dissociation of phosphatidic acid in small unilamellar vesicles - a <sup>31</sup>P-NMR study. *Biochim. Biophys. Acta, Biomembr.* **1994**, *1191*, 354–361.

(34) Smart, J. L.; McCammon, J. A. Surface titration: A continuum electrostatics model. *J. Am. Chem. Soc.* **1996**, *118*, 2283–2284.

(35) Sakurai, M.; Tamagawa, H.; Inoue, Y.; Ariga, K.; Kunitake, T. Theoretical study of intermolecular interaction at the lipid–water interface. 1. Quantum chemical analysis using a reaction field theory. *J. Phys. Chem. B* **1997**, *101*, 4810–4816.

(36) Tamagawa, H.; Sakurai, M.; Inoue, Y.; Ariga, K.; Kunitake, T. Theoretical study of intermolecular interaction at the lipid–water interface. 2. Analysis based on the Poisson–Boltzmann equation. *J. Phys. Chem. B* **1997**, *101*, 4817–4825.

(37) Ma, M.; Bong, D. Directed peptide assembly at the lipid–water interface cooperatively enhances membrane binding and activity. *Langmuir* **2010**, *27*, 1480–1486.

(38) Schulz, M.; Glatte, D.; Meister, A.; Scholtysek, P.; Kerth, A.; Blume, A.; Bacia, K.; Binder, W. H. Hybrid lipid/polymer giant unilamellar vesicles: effects of incorporated biocompatible PIB-PEO block copolymers on vesicle properties. *Soft Matter* **2011**, *7*, 8100–8110.

(39) Binder, W. H. Polymer-induced transient pores in lipid membranes. *Angew. Chem., Int. Ed.* **2008**, *47*, 3092–3095.

(40) Meier, W.; Ruyschaert, T.; Sonnen, A. F. P.; Haefele, T.; Winterhalter, M.; Fournier, D. Hybrid nanocapsules: Interactions of ABA block copolymers with liposomes. *J. Am. Chem. Soc.* **2005**, *127*, 6242–6247.

(41) Meier, W.; Kita-Tokarczyk, K.; Ite, F.; Grzelakowski, M.; Egli, S.; Rossbach, P. Interactions between lipids and amphiphilic block copolymers. *Langmuir* **2009**, *25*, 9847–9856.

(42) Nam, J.; Beales, P. A.; Vanderlick, T. K. Giant phospholipid/block copolymer hybrid vesicles: mixing behavior and domain formation. *Langmuir* **2011**, *27*, 1–6.

(43) Lecommandoux, S.; Sandre, O.; Chécot, F.; Perzynski, R. Smart hybrid magnetic self-assembled micelles and hollow capsules. *Prog. Solid State Chem.* **2006**, *34*, 171–179.

(44) Schulz, M.; Werner, S.; Bacia, K.; Binder, W. H. Controlling molecular recognition with lipid/polymer domains in vesicle membranes. *Angew. Chem., Int. Ed.* **2013**, *52*, 1829–1833.

(45) Schulz, M.; Olubummo, A.; Binder, W. H. Beyond the lipid-bilayer: interaction of polymers and nanoparticles with membranes. *Soft Matter* **2012**, *8*, 4849–4864.

(46) Olubummo, A.; Schulz, M.; Lechner, B.-D.; Scholtysek, P.; Bacia, K.; Blume, A.; Kressler, J.; Binder, W. H. Controlling the localization of polymer-functionalized nanoparticles in mixed lipid/polymer membranes. *ACS Nano* **2012**, *6*, 8713–8727.

(47) Sachsenhofer, R.; Binder, W. H.; Farnik, D.; Zirbs, R. Polymersome-embedded nanoparticles. *Macromol. Symp.* **2007**, *254*, 375–377.

(48) Binder, W. H.; Sachsenhofer, R.; Farnik, D.; Blaas, D. Guiding the location of nanoparticles into vesicular structures: a morphological study. *Phys. Chem. Chem. Phys.* **2007**, *9*, 6435–6441.

(49) Binder, W. H.; Barragan, V.; Menger, F. M. Domains and rafts in lipid membranes. *Angew. Chem., Int. Ed.* **2003**, *42*, S802–S827.

(50) Adekunle, O.; Herbst, F.; Hackethal, K.; Binder, W. H. Synthesis of nonsymmetric chain end functionalized polyisobutylenes. *J. Polym. Sci., Polym. Chem.* **2011**, *49*, 2931–2940.

(51) Binder, W. H.; Lomoschitz, M.; Friedbacher, G.; Sachsenhofer, R. Reversible and irreversible binding of nanoparticles to polymeric surfaces. *J. Nanomater.* **2009**, DOI: 10.1155/2009/613813.

(52) Skaff, H.; Ilker, M. F.; Coughlin, E. B.; Emrick, T. Preparation of cadmium selenide–polyolefin composites from functional phosphine oxides and ruthenium-based metathesis. *J. Am. Chem. Soc.* **2002**, *124*, 5729–5733.

(53) Uyeda, H. T.; Medintz, I. L.; Jaiswal, J. K.; Simon, S. M.; Mattoussi, H. Synthesis of compact multidentate ligands to prepare stable hydrophilic quantum dot fluorophores. *J. Am. Chem. Soc.* **2005**, *127*, 3870–3878.

(54) Attwood, S.; Choi, Y.; Leonenko, Z. Supported planar lipid bilayers for atomic force microscopy and atomic force spectroscopy. *Int. J. Mol. Sci.* **2013**, *14*, 3514–3539.

(55) Breslow, R.; Zhang, B. Cholesterol recognition and binding by cyclodextrin dimers. *J. Am. Chem. Soc.* **1996**, *118*, 8495–8496.

(56) Jing, B.; Zhu, Y. E. Disruption of supported lipid bilayers by semi-hydrophobic nanoparticles. *J. Am. Chem. Soc.* **2011**, *133*, 10983–10989.

(57) Chen, J.; Hessler, J. A.; Khan, D. P.; Som, A.; Hong, S.; Tew, G. N.; Holl, M. M. B.; Putchakayala, K.; Mullen, D. G.; Lopatin, A. N.; Orr, G. B.; Panama, B. K.; DiMaggio, S. C.; Baker, J. R. Cationic nanoparticles induce nanoscale disruption in living cell plasma membranes. *J. Phys. Chem. B* **2009**, *113*, 11179–11185.

(58) Walde, P.; Cosentino, K.; Engel, H.; Stano, P. Giant vesicles: preparations and applications. *ChemBioChem* **2010**, *11*, 848–865.

(59) Sackmann, E. Membrane bending energy concept of vesicle- and cell-shapes and shape-transitions. *FEBS Lett.* **1994**, *346*, 3–16.

(60) Baumgart, T.; Hess, S. T.; Webb, W. W. Imaging coexisting fluid domains in biomembrane models coupling curvature and line tension. *Nature* **2003**, *425* (6960), 821–824.